Particle layering in the ceramic-metal thin film Pt-Al_2O_3

A. Gibaud,[1] S. Hazra,[1] C. Sella,[2] P. Laffez,[1] A. Désert,[1] A. Naudon,[3] and G. Van Tendeloo[4]
[1]*Laboratoire de Physique de l'Etat Condensé, UPRES A 6087 CNRS, Faculté des Sciences, Université du Maine, 72085 Le Mans, France*
[2]*Laboratoire d'Optique des Solides, Université de Paris VI, Case 80, 4 Place Jussieu, 75252 Paris, France*
[3]*Laboratoire de Métallurgie Physique, UMR 6630 CNRS, Université de Poitiers, 86960 Futuroscope, France*
[4]*EMAT, University of Antwerp (RUCA), Groenenborgerlaan 171, B-2020, Antwerp, Belgium*
(Received 11 July 2000; revised manuscript received 10 January 2001; published 25 April 2001)

Experiments performed by x-ray reflectivity, grazing incidence small angle x-ray scattering (GISAXS), and transmission electron microscopy (TEM) on a cosputtered nanocermet thin film of Pt-Al_2O_3 are presented. It is shown that the morphology of such a heterogeneous material can be well interpreted by combining the information obtained from the three techniques. In particular, the layering of metal nanoparticles in the immediate vicinity of the substrate is clearly evidenced. GISAXS results are interpreted via a model which yields spherical nanoparticles of diameter $2R=3.1$ nm, separated on the average by a distance of 5.8 nm. The evidence for the layering of particles close to the substrate is deduced from the analysis of the specular reflectivity and probed directly by TEM.

DOI: 10.1103/PhysRevB.63.193407 PACS number(s): 68.55.−a, 61.10.Kw, 68.37.Lp, 61.46.+w

Ceramic metal (cermet) thin films are presenting considerable interest as useful devices to absorb radiation in the visible and near infrared region of solar spectrum. They have already been used in solar plants and they could be used in the future as smart coatings for windows or as nonlinear optical devices. It is now well known that cermets are made of metal nanoparticles which can coexist in an insulator matrix such as alumina (Al_2O_3) or silica (SiO_2) in any proportion. The presence of such confined metal particles in dielectric matrix changes the physical properties of the system.[1–3] Cermets absorb the radiation of solar spectrum mainly because of their heterogeneous structure and for this reason the determination of the structure and morphology is becoming increasingly important. Recently, grazing incidence small angle x-ray scattering (GISAXS) has proved to be invaluable for analyzing both the size distribution and the spatial location of nanoobjects in directions parallel and perpendicular to the surface of the film with the exception of the specular direction.[4] Up to now, the complete structure of such films remains unknown mainly because the arrangement of the metal particles in the direction normal to the surface (called the z direction) is not yet understood. In thin films, metal particles are confined in the z-direction so that their spatial repartition along this direction can be fairly different from the in-plane one. In addition, the morphology of these films may differ from one region to the next so that only a statistical approach is relevant.[5] In confined geometry, layering of particles or molecules close to interfaces has been recently reported in different systems such as liquid metals, polymer, and in molecular liquids deposited on a flat substrate.[6–10] In liquid metals, the layering occurs at the liquid-air interface whereas in the recent study of thin films of tetrakis (2-ethylhexoxy) silane, the layering of the molecules was found at the solid-liquid interface. The technique which is used to probe the layering in both cases is x-ray reflectometry. Indeed, such a technique is undisputed to determine the electron density profile (EDP) in the z direction, normal to the surface of thin films. In particular, it is possible in the case of weakly interacting materials to interpret normalized specular x-ray reflectivity data R/R_F (R_F is the absolute reflectivity of the substrate) as the Fourier transform of the Patterson function $P(z)$ of the derivative of the electron density. It can be shown that

$$P(z)=\int \frac{\partial\rho(z+s)}{\partial s}\frac{\partial\rho(s)}{\partial s}ds \Rightarrow \frac{R(q_z)}{R_F(q_z)}=\mathrm{FT}[P(z)]. \tag{1}$$

The signature of the layering is obvious when oscillations having nothing to do with the finite thickness of the film are observed in the normalized *true* specular reflectivity. Since the Patterson function just gives the mean distance between immediate neighbors but does not give the exact location of the molecules or particles involved in the layering, direct probes are then necessary to strengthen the conclusions drawn from x-ray reflectivity analysis. In particular, when one comes to define the exact location of the layering, such probes are essential. In liquids, direct structural probes which have been used to evidence the layering are the measurements of the force between two mica plates separated by the molecular liquid, ellipsometric measurements, and computer simulations. So far, the layering in cermets has been inferred by x-ray measurements[11,12] but has never been evidenced directly. In such solid thin films the use of transmission electron microscopy (TEM) to directly probe the layering was therefore particularly appealing with the main difficulty to produce a cross section of the thin film. It is the purpose of this paper to present the combined study of the TEM, GISAXS, and specular reflectivity measurements of a thin film of cermet made of Pt clusters inserted in an amorphous matrix of alumina deposited on a silicon substrate. Complementary experiments made on similar films deposited on other substrates are also presented to straighten the proof of the layering.

The cermet thin film was made by cosputtering Pt and alumina (small pellets of Pt were placed in an alumina disk)

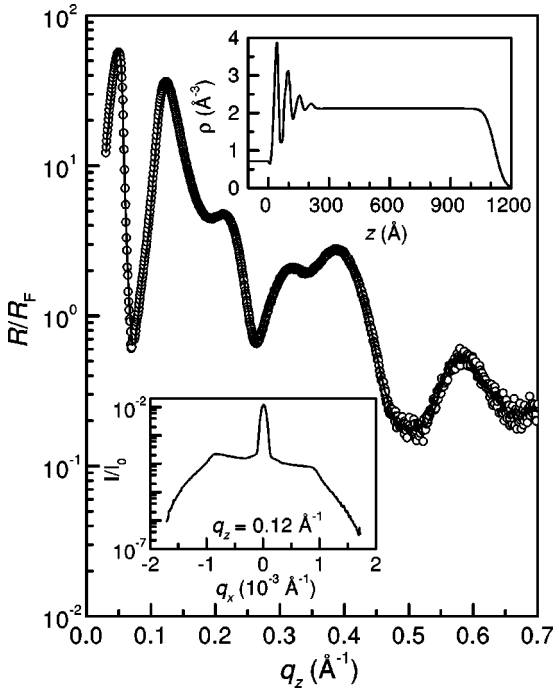

FIG. 1. Observed (open circles) and calculated (solid line) normalized x-ray reflectivity curves of Pt-Al_2O_3 nanocermet thin film deposited on a silicon substrate. The electron density profile and a transverse scan parallel to the surface of the sample taken at $q_z = 0.12$ Å^{-1} are displayed in the insets.

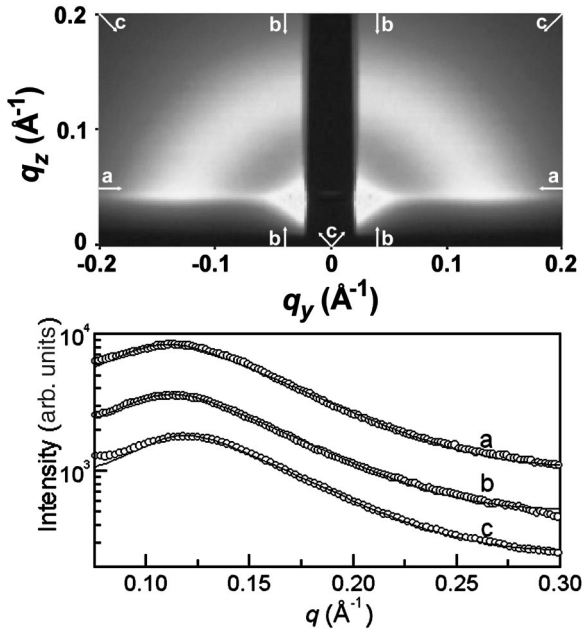

FIG. 2. GISAXS image of Pt-Al_2O_3 nanocermet thin film. Three line profiles (open circles) drawn through the image in different direction are shown in bottom. Solid lines are the calculated profiles according to the model discussed in the text.

onto the surface of a Si(001) wafer. The Si substrate was rotated during the deposition to ensure the homogeneity of the thin film and was held at a temperature of 300 °C.

X-ray reflectivity and diffuse scattering measurements of the thin film were performed using laboratory source at wavelength $\lambda = 1.54$ Å. X-ray measurements were performed in reflection geometry, first in the specular condition and then completed by off-specular scans. Wide angle measurements were also performed which show the amorphous nature of the insulator and the crystalline state of the metallic inclusions. GISAXS measurements of the thin film were carried out (on the D22 beam line of LURE, Orsay) at a fixed energy of 7 keV with a two-dimensional (2D) wire detector. The incident angle was fixed to a value slightly above the critical angle and the specular reflected beam was masked to avoid the saturation of the detector. At this angle, we estimate that the penetration depth (defined as the distance corresponding to an attenuation of $1/e$) is of the order of 1250 Å.

Microstructural characterization of the thin film was performed using high resolution transmission electron microscope (Philips CM30-FEG with ultra-twin lens working at 300 kV, Scherzer resolution 1.6 Å). Cross-sectional foils [which are parallel to (110) plane of the Si substrate] used for the TEM measurements were prepared from the thin film by mechanical polishing and ion milling. Imaging was performed along the [110] axis of the silicon substrate and the images were analyzed using the NIH image program.

Figure 1 shows the normalized reflectivity data (R/R_F) from the Pt-Al_2O_3 cermet thin film. One can clearly observe a steep decrease of the intensity which corresponds to the critical angle followed by a number of broad peaks which are related to the layering of the Pt clusters. In particular there is a dominant peak at $q_z = 0.12$ Å^{-1} which is also observed in the longitudinal (not shown here) diffuse scan and in the GISAXS measurement shown in Fig. 2. The transverse scan (inset of Fig. 1), shows that the dominant peak has a resolution-limited component which corresponds to true specular scattering. In Fig. 2, one can clearly observe a ring, the radius of which gives the average distance between particles and the width of which is related to both the distance and the size of the particles. We naturally attribute this peak to the average distance between particles both in the specular and in the off-specular directions. Since it is much more intense in the specular reflectivity than in the diffuse scattering (see inset of Fig. 1 where the flat part is part of the ring), we consider that we have here the signature of the layering of particles in the z direction. The fact that this peak is found at the same position in both scans indicates that the distance between the particles is about the same in the z direction than in the plane of the film. The observation of a ring clearly proves the existence of an average distance between the particles whatever the considered direction.

In order to get a more quantitative picture of the structural arrangement, we have considered that this heterogeneous film could be nevertheless separated in slabs of different electron densities in the following way. Starting from the silicon substrate, the film is decomposed in an oxide, followed by a region of about 300 Å in which the electron density is oscillating due to the presence of the layering (region 1), then in a region in which the particles do not present a specific ordering along the z direction (region 2) and finally terminated by the rough film-air interface. The region 2

where there is no ordering along the z direction is heterogeneous on a microscopic scale but homogeneous when averaged over the size of the x-ray probe. This region contributes essentially to the diffuse ring $I_D(q)$ which is observed in the GISAXS measurements (here q is the modulus of the wave vector transfer and to the diffuse intensity observed in the longitudinal off-specular diffuse scattering). It also dictates the average electron density of the film. On the contrary, the interfaces between the silicon substrate, the oxide, the layered region (region 1), region 2, and air contribute to the specular reflectivity $R(q_z)$ where q_z is the wave vector transfer along the normal to the surface of the film. Indeed at each of these interfaces, the derivative of the electron density when averaged over the size of the beam is peaked. Therefore the total intensity can written as

$$I(\vec{q}) = R(q_z) + I_D(q). \tag{2}$$

The diffuse intensity is calculated analytically via a cumulative disorder process[13] and the specular reflectivity is determined by the matrix technique. Assuming spherical particles of mean radius R, separated on the average by a distance d with a mean deviation σ_d, one can show that the diffuse scattering yields

$$I_D(q) = A \frac{[\sin(qR) - qR\cos(qR)]^2}{(qR)^6} \times \frac{1 - e^{-2q^2\sigma_d^2}}{1 - 2e^{-q^2\sigma_d^2}\cos(qd) + e^{-2q^2\sigma_d^2}}. \tag{3}$$

This description was improved by including in a numerical way a distribution of radii with a Gaussian probability of variance σ_R. The scale factor A includes the contrast of electron density between the metallic particles and the insulating matrix, the particle concentration, and instrumental geometrical parameters. The best fit of the reflectivity curve and the corresponding EDP are shown in Fig. 1. The EDP which is obtained from the specular reflectivity analysis only, shows that the total film thickness is about 1200 Å (oscillations barely visible in Fig. 1 are used to determine this thickness) and that the top surface roughness, $\sigma = 34$ Å, is very large. The oscillations in the EDP are characteristic of the average interparticle distance in the first layers of the film. This distance is found to be 58 Å. The diffuse intensity presented in Eq. (3) is used to fit the GISAXS line profile along different directions as shown in the bottom of Fig. 2. The relevant parameters that are obtained from the fit are the radius R of the particles, the interparticle distance d and the variance of these distributions. The values of these parameters are $2R = 31 \pm 5$ Å, $d = 58 \pm 8$ Å, $\sigma_d = 8$ Å.

Although this model is in fairly good agreement with the experimental x-ray data, we have performed TEM measurements on a cross section of the film to plainly validate it. The TEM picture is presented in Fig. 3 and confirms beautifully the presented model. One can clearly observe in this figure the ordering of the particles (region 1) located immediately above the oxide layer covering the silicon substrate and above a region (region 2) where the particles are separated

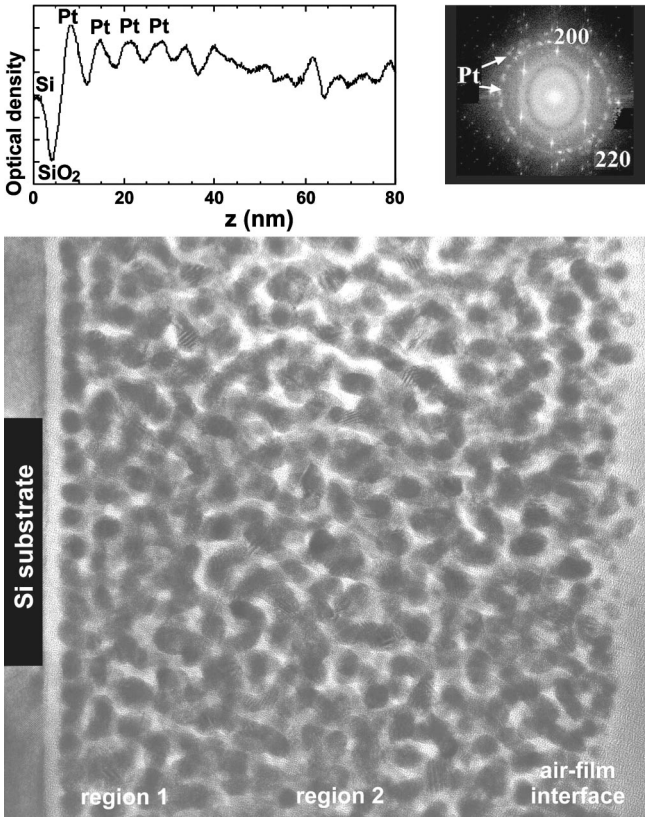

FIG. 3. Cross-sectional TEM image of Pt-Al_2O_3 nanocermet thin film. Dark regions correspond to the Pt clusters and white regions to the amorphous Al_2O_3 matrix. The layering of Pt particles is obvious in the immediate vicinity of the substrate (region 1) and quickly vanishes after a few layers to give rise to a film of uniform electron density. The top part of the figure shows the optical density of the image along the growth direction together with the scale. In the FFT of the image which is shown in the inset, one can clearly observe rings of scattering due to crystalline Pt regions and well-defined spots coming from the Si substrate.

from each others but do not present any particular ordering in the z direction. The thickness of the film is estimated around 1200 Å and the roughness of the air-film interface is obviously very large. The Fourier transformation of the TEM picture shows a rectangular lattice corresponding to the silicon substrate and two rings at 2.25 and 1.96 Å, respectively. These two distances correspond to the interplanar distance of Pt and confirm the crystallization of this phase. However, each diffraction ring is fairly broad, which can be related to local lattice deformation within the Pt particles. Within each Pt particle, a high density of planar defects is evidenced.[14] The average diameter of the particles was obtained assuming spherical particles and was found to be 35 Å. Optical density profile was calculated for different areas of the sample, perpendicular to the substrate by averaging the optical density in the direction parallel to the substrate. For the calculation a depth of 800 Å was selected and the average intensity value was measured in a 780 Å length. In our digitization process, black dots are set arbitrarily to 255 and white dots to 0. A typical optical density profile for an area of the sample is shown in Fig. 3. The origin is taken at the silicon substrate

(labeled on the figure). One first observes a minimum of the average optical density that corresponds to the SiO_2 amorphous layer. The optical density then increases and reaches a maximum, which is suggested to be the first platinum particle layer. Then the optical density shows oscillations with a succession of minima and maxima. This behavior is clearly established up to 400 Å. An average pseudoperiod of 57 Å was estimated for the position of the maxima, when moving from the silicon toward the top of substrate. This value is comparable with the average separation between Pt particles found from x-ray reflectivity and GISAXS analyses.

It is important to note that the layering also appears when the cermet thin film is deposited on different kind of flat substrates such as float glass, for example. The results of some complementary experiments were found to be easy to interpret once the layering was firmly established. In particular, we have evidenced that the ratio between the intensity of the specular hump located at $q_z = 0.12$ Å^{-1} and that of the ring becomes fainter for very thick films. This is fully expected since the layering region becomes buried under a thick heterogeneous film. In addition when varying the roughness of the substrate by mechanical polishing, we have observed that for films of identical thickness (about 1000 Å), the specular component becomes less and less intense for higher roughness. This component can even completely vanish for severe alteration of the substrate surface. Nevertheless the off-specular signal remains similar in all cases (a detailed description of this experiment will appear soon).

In conclusion, we have shown that thin films of cermets made from Pt nanoparticles dispersed in an amorphous matrix of alumina present a heterogeneous structure in the direction normal to the surface of the film. In particular, the morphology of the film consists of layers of Pt particles located in the immediate vicinity of the substrate followed by a region where the alignment of the particles parallel to the substrate is completely relaxed. The complete understanding of such a complex morphology, from experimental point of view, was made possible by combining the three complementary techniques: TEM, GISAXS, and x-ray reflectivity. The layering was shown by the combined analysis of the GISAXS and x-ray reflectivity and then confirmed by TEM. From a theoretical point of view, the formation of metal thin films proceeds via nucleation, growth and coalescence.[15] There are different models for the nucleation such as capillary, kinetic, Walton-Rhodin, etc. Similarly, coalescence can take place by Ostwald ripening, sintering or cluster migration. In the case of a sequential deposition of cobalt and alumina,[16] GISAXS can demonstrate that there is a well defined in-plane local order of the Co clusters as well as a vertical organization. For the cosputtered cermets, the growth mechanism of metal particles in the dielectric ceramic remains unknown. It is likely that the nucleation of metal atoms in the cermet thin film will be further controlled by the temperature, the ceramic atmosphere, and the metal-ceramic sputtering ratio. Similarly, metal particles can only grow to a certain extent in presence of ceramic matrix and the size and shape of the particles will be such that it will minimize the energy of the system by optimizing the surface free energy. Separated particles in cermet thin films, below the percolation threshold, is well expected.[1,3] However, the formation of layering of particles in cosputtered thin films has never been observed before.

The authors wish to thank the LURE for access to the D22 beam line and are greatly indebted to O. Lyon. This work was supported by the Microcap-Ouest project.

[1] B. Abeles, P. Shing, M.D. Coutts, and Y. Arie, Adv. Phys. **24**, 407 (1975).
[2] G.A. Niklasson and C.G. Grandqvist, J. Appl. Phys. **55**, 3382 (1984).
[3] W.P. Halperin, Rev. Mod. Phys. **58**, 533 (1986).
[4] A. Naudon and D. Babonneau, Z. Metallkd. **88**, 596 (1997).
[5] A. Gibaud, C. Sella, M. Maaza, L. Sung, J.A. Dura, and S.K. Satija, Thin Solid Films **340**, 153 (1999).
[6] O.M. Magnussen, B.M. Ocko, M.J. Regan, K. Penanen, P.S. Pershan, and M. Deutsch, Phys. Rev. Lett. **74**, 4444 (1995).
[7] M.J. Regan, E.H. Kawamoto, S. Lee, P.S. Pershan, N. Maskil, M. Deutsch, O.M. Magnussen, B.M. Ocko, and L.E. Berman, Phys. Rev. Lett. **7**, 2498 (1995).
[8] M.K. Sanyal, J.K. Basu, A. Datta, and S. Banerjee, Europhys. Lett. **36**, 265 (1996).
[9] W.J. Huisman, J.F. Peters, M.J. Zwanenburg, S.A. de Vries, T.E. Derry, D. Abernathy, and J.F. Van der Veen, Nature (London) **390**, 379 (1997).
[10] C.J. Yu, A.G. Richter, A. Datta, M.K. Durbin, and P. Dutta, Phys. Rev. Lett. **82**, 2326 (1999).
[11] S. Hazra, A. Gibaud, P. Laffez, and C. Sella, Eur. Phys. J. B **14**, 363 (2000).
[12] S. Hazra, A. Gibaud, A. Desert, C. Sella, and A. Naudon, Physica B **283**, 97 (2000).
[13] B.K. Vainshtain, *Diffraction of X-rays by Chain Molecules* (Elsevier, Amsterdam, 1966).
[14] Details HRTEM and EELS studies are in progress to understand the particles structure and the particle-matrix interface.
[15] M. Ohring, *The Materials Science of Thin Films* (Academic Press, San Diego, 1992).
[16] D. Babonneau, F. Petroff, J.L. Maurice, F. Fettar, A. Vaurès, and A. Naudon, Appl. Phys. Lett. **76**, 2892 (2000).